Molecular Therapy
Nucleic Acids
Original Article

Recurrence-Associated Long Non-coding RNA LNAPPCC Facilitates Colon Cancer Progression via Forming a Positive Feedback Loop with PCDH7

Ting Li,[1,7] Zhiqiang Li,[2,7] Hongxing Wan,[2] Xifeng Tang,[2] Han Wang,[3] Fang Chai,[4] Meng Zhang,[5] and Baochun Wang[6]

[1]Department of Gastroenterology, Sanya People's Hospital, Sanya, Hainan, China; [2]Department of Surgical Oncology, Sanya People's Hospital, Sanya, Hainan, China; [3]Department of Pathology, Sanya People's Hospital, Sanya, Hainan, China; [4]Department of Pharmacy, Sanya People's Hospital, Sanya, Hainan, China; [5]Department of Radiology, Sanya People's Hospital, Sanya, Hainan, China; [6]Department of General Surgery, Hainan General Hospital, Hainan Affiliated Hospital to Hainan Medical University, Haikou, Hainan, China

Long non-coding RNAs (lncRNAs) gradually show critical regulatory roles in many malignancies. However, the lncRNAs implicated in colon cancer recurrence are largely unknown. In this study, we searched the lncRNAs associated with metastasis and recurrence of colon cancer using GEO datasets. We focused on a novel lncRNA long non-coding RNA associated with poor prognosis of colon cancer (LNAPPCC), which is highly expressed in colon cancer. Increased expression of LNAPPCC is positively associated with metastasis, recurrence, and poor survival of colon cancer patients. LNAPPCC promotes colon cancer cell proliferation, migration, and *in vivo* xenograft growth and liver metastasis. Mechanistic investigations revealed that LNAPPCC binds EZH2, represses the binding of EZH2 to *PCDH7* promoter, downregulates histone H3K27me3 level in *PCDH7* promoter, and activates *PCDH7* expression. Intriguingly, we also found that PCDH7 activates ERK/c-FOS signaling, increases the binding of c-FOS to *LNAPPCC* promoter, and activates *LNAPPCC* expression. Therefore, LNAPPCC and PCDH7 form a positive regulatory loop via EZH2 and ERK/c-FOS. The positive correlations between the expression of LNAPPCC, PCDH7, phosphorylated ERK, and phosphorylated c-FOS are detected in colon cancer tissues. Furthermore, depletion of PCDH7 or the adding of ERK inhibitor abolished the oncogenic roles of LNAPPCC in colon cancer. In summary, this study identified a novel lncRNA LNAPPCC that is highly expressed in colon cancer and associated with poor prognosis of colon cancer patients. LNAPPCC exerts oncogenic roles in colon cancer via forming a positive feedback loop with PCDH7. Targeting LNAPPCC/EZH2/PCDH7/ERK/c-FOS signaling axis represents a potential therapeutic strategy for colon cancer.

INTRODUCTION

Colon cancer, which originates from malignant transformation of colonic epithelial cells, has become a severe public health threat due to the high incidence and mortality worldwide.[1,2] There were 1,096,601 estimated new cases and 551,269 estimated deaths of colon cancer in 2018 globally.[2] In 2019 cancer statistics in the United States, colon cancer ranked third in both incidence and mortality.[3] Despite great advances that have been made in surgical resection, chemotherapy, immunotherapy, and so on, the prognosis of about 30% of colon cancer patients is still very poor due to recurrence and/or metastasis.[4,5] Therefore, revealing the critical molecular events underlying colon cancer recurrence and metastasis to develop more efficient prognostic biomarkers and therapeutic targets is urgently demanded.[6,7]

The advances of genome and transcriptome high-throughput sequencing have found that the human genome encodes more non-coding RNAs than mRNAs.[8–10] Among these non-coding RNAs, long non-coding RNA (lncRNA) is a class of transcripts more than 200 nucleotides in length with limited protein coding potential.[11–15] Increasing evidence has demonstrated that lncRNAs are frequently involved in the initiation and progression of various cancers, including colon cancer.[16–21] For example, upregulated lncRNA ITIH4-AS1 promotes proliferation and metastasis of colon cancer via activating JAK/STAT3.[22] lncRNA LINC02418 is highly expressed and may be a diagnostic biomarker for colon cancer.[23] lncRNA CALIC accelerates colon cancer metastasis via upregulating AXL.[24] Although several lncRNAs have been identified to be aberrantly expressed and play corresponding biological roles in colon cancer, the lncRNAs with a predictive value of recurrence and metastasis of colon cancer are still lacking.

In the present study, using gene expression signatures of colon cancers from GEO datasets (https://www.ncbi.nlm.nih.gov/gds/), we

Received 14 February 2020; accepted 30 March 2020;
https://doi.org/10.1016/j.omtn.2020.03.017.

[7]These authors contributed equally to this work.

Correspondence: Baochun Wang, Department of General Surgery, Hainan General Hospital, Hainan Affiliated Hospital to Hainan Medical University, Haikou, Hainan, China.
E-mail: baochun_wang@163.com

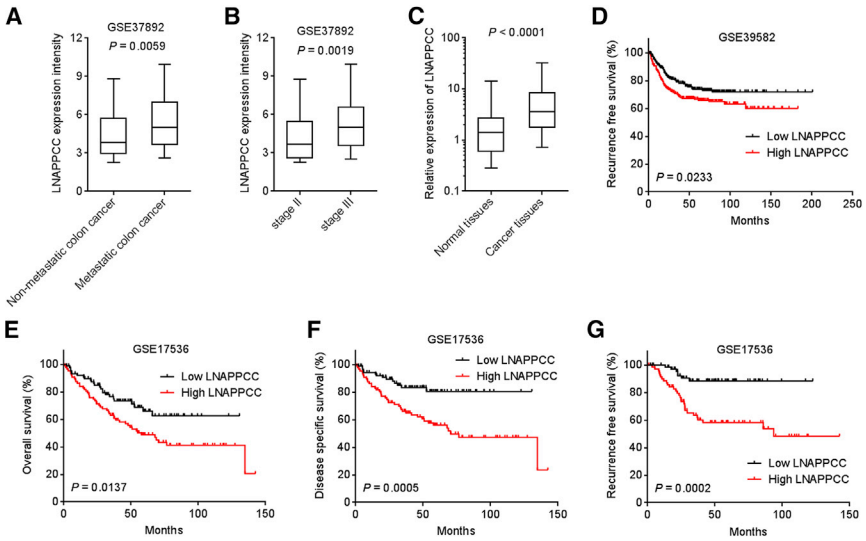

Figure 1. Expression Pattern and Clinical Significances of LNAPPCC

(A) LNAPPCC expression intensities in 93 non-metastatic and 37 metastatic colon cancer tissues from GSE37892 data. p = 0.0059 by Mann-Whitney test. (B) LNAPPCC expression intensities in 73 stage II and 57 stage III colon cancer tissues from GSE37892 data. p = 0.0019 by Mann-Whitney test. (C) LNAPPCC expression levels in 62 pairs of colon cancer tissues and matched adjacent normal tissues were detected by quantitative real-time PCR. p < 0.0001 by Wilcoxon matched-pairs signed rank test. (D) Kaplan-Meier survival analysis of the correlation between LNAPPCC expression intensities and recurrence free survival from GSE39582 data. n = 577, p = 0.0233 by log-rank test. (E) Kaplan-Meier survival analysis of the correlation between LNAPPCC expression intensities and overall survival from GSE17536 data. n = 177, p = 0.0137 by log-rank test. (F) Kaplan-Meier survival analysis of the correlation between LNAPPCC expression intensities and disease specific survival from GSE17536 data. n = 177, p = 0.0005 by log-rank test. (G) Kaplan-Meier survival analysis of the correlation between LNAPPCC expression intensities and recurrence free survival from GSE17536 data. n = 145, p = 0.0002 by log-rank test.

identified a novel lncRNA (GenBank: AK095791), which may predict metastasis and poor prognosis of colon cancer. Therefore, we termed this lncRNA as long non-coding RNA associated with poor prognosis of colon cancer (LNAPPCC). We further investigated the expression pattern and clinical significance of LNAPPCC in colon cancer. Furthermore, gain- and loss-of-function experiments were undertaken to explore the roles of LNAPPCC in colon cancer. Mechanistic investigation identified a positive feedback loop between LNAPPCC, PCDH7, ERK, and c-FOS, which mediate the oncogenic roles of LNAPPCC in colon cancer.

RESULTS

LNAPPCC Is Highly Expressed in Colon Cancer and High Expression of LNAPPCC Is Correlated with Metastasis and Poor Prognosis of Colon Cancer Patients

To search the lncRNAs involved in colon cancer metastasis, we compared the differentially expressed genes from GSE37892 data, which includes 93 non-metastatic and 37 metastatic colon cancer tissues using GEO2R. Among these differentially expressed genes shown in Table S1, LNAPPCC (probe ID: 232113_at) is the most remarkably upregulated lncRNA with the largest fold-change (FC) value in metastatic colon cancer tissues compared with non-metastatic colon cancer tissues (Figure 1A). Analyzing the provided clinicopathological characteristics of these 130 colon cancer patients from GSE37892, we found that LNAPPCC expression intensity is higher in stage III colon cancer compared with stage II colon cancer (Figure 1B). LNAPPCC expression intensity is not correlated with age and tumor location (Figures S1A and S1B). The expression of LNAPPCC in 62 pairs of colon cancer tissues and matched adjacent normal tissues was further measured by quantitative real-time PCR. The results found that LNAPPCC is remarkably highly expressed in colon cancer tissues compared with normal tissues (Figure 1C). Correlation analyses of LNAPPCC expression and clinicopathological characteristics in these 62 colon cancer cases revealed that high expression of LNAPPCC is positively correlated with advanced tumor node metastasis (TNM) stages, but not correlated with age and sex (Table 1). Compared with normal human colon mucosal epithelial cell line NCM460, the expression of LNAPPCC is also remarkably increased in colon cancer cell lines HT-29, SW620, HCT-15, and HCT116 (Figure S1C). Kaplan-Meier survival analysis was undertaken using GSE39582 and GSE17536 data to detect the correlation between LNAPPCC expression and prognosis. As shown in Figure 1D, high expression of LNAPPCC is correlated with poor recurrence-free survival in GSE39582 data. Moreover, high expression of LNAPPCC is remarkably correlated with poor overall survival, poor disease specific survival, and more cancer recurrence (Figures 1E–1G). LNAPPCC is mainly located in the nucleus and poly(A)-positive (Figures S1D and S1E). LNAPPCC full-length sequence was determined with 5′ and 3′ rapid amplification of cDNA ends (RACE) and shown in Figure S1F. Open reading frame (ORF) finder from the National Center for Biotechnology Information (https://www.ncbi.nlm.nih.gov/orffinder/) and codon substitution frequency analysis using PhyloCSF calculation on UCSC Genome Browser (http://genome.ucsc.edu) both showed that LNAPPCC is a non-coding RNA (Figures S1G and S1H).

LNAPPCC Facilitates Colon Cancer Cell Proliferation and Migration

To observe the potential functions of LNAPPCC in colon cancer, we constructed LNAPPCC stably overexpressed HCT116 and SW620 cells via stable transfection of LNAPPCC mammalian expression plasmid pcDNA/LNAPPCC (Figures 2A and 2B). Cell counting kit-8 (CCK-8) assays revealed that cell proliferation of both HCT116 and SW620 cells was remarkably increased by LNAPPCC

Table 1. Correlation between LNAPPCC Expression and Clinicopathological Characteristics

Variable	LNAPPCC		p Value
	Low	High	
Age			0.442
>60	16	19	
≤60	15	12	
Sex			0.445
Male	13	16	
Female	18	15	
Pathology T stage			0.029
T1-2	10	3	
T3-4	21	28	
Pathology N Stage			0.030
N0	25	17	
N1-2	6	14	
Pathology M stage			0.038
M0	29	23	
M1	2	8	

p value was calculated by Pearson chi-square test.

overexpression (Figures 2C and 2D). The pro-proliferative roles of LNAPPCC were further confirmed by 5-ethynyl-2′-deoxyuridine (EdU) incorporation assay (Figure 2E). Transwell assays revealed that cell migration of both HCT116 and SW620 cells was remarkably increased by LNAPPCC overexpression (Figure 2F). To further confirm the oncogenic roles of LNAPPCC, we stably overexpressed LNAPPCC in normal human colon mucosal epithelial cell line NCM460 (Figure S2A). CCK-8 and EdU incorporation assays revealed that overexpression of LNAPPCC also promoted NCM460 cell proliferation (Figures S2B and S2C). Transwell assays revealed that overexpression of LNAPPCC also promoted NCM460 cell migration (Figure S2D). LNAPPCC stably silenced HCT116 cells were constructed via stable transfection of two independent LNAPPCC-specific short hairpin RNAs (shRNAs; Figure 2G). Both CCK-8 and EdU incorporation assays revealed that cell proliferation was remarkably repressed by silencing of LNAPPCC (Figures 2H and 2I). Furthermore, Transwell assays revealed that cell migration was also remarkably repressed by silencing of LNAPPCC (Figure 2J). Collectively, these findings suggested that LNAPPCC plays oncogenic roles in colon cancer.

The Expression of LNAPPCC Is Significantly Positively Correlated with that of PCDH7, Whose High Expression Is Also Associated with Metastasis and Poor Prognosis of Colon Cancer Patients

Next, we investigated the molecular mechanisms mediating the oncogenic roles of LNAPPCC in colon cancer. The candidate targets of LNAPPCC were searched based on the following criteria: (1) the targets are differentially expressed between metastatic and non-metastatic colon cancer tissues from GSE37892 data; (2) the expression of the targets is correlated with LNAPPCC in colon cancer tissues from GSE37892 data; and (3) the expression of the targets is correlated with LNAPPCC in colon cancer tissues from GSE17536 data. Following the above criteria, we identified 13 candidates (Table S2). Among these candidates, we noted PCDF7 (probe ID: 228640_at), which has been reported to modulate tumor metastasis.[25–27] Consistent with LNAPPCC, PCDH7 is also remarkably increased in metastatic colon cancer tissues compared with non-metastatic colon cancer tissues from GSE37892 data (Figure 3A). The expression of PCDH7 is remarkably positively correlated with LNAPPCC from both GSE37892 and GSE17536 data, with R value of 0.7844 and 0.6865, respectively (Figures 3B and 3C). Furthermore, Kaplan-Meier survival analysis showed that consistent with LNAPPCC, high expression of PCDH7 is remarkably correlated with poor overall survival, poor disease specific survival, and more cancer recurrence from GSE17536 data (Figures 3D–3F). The positive correlation between the expression of PCDH7 and LNAPPCC was further confirmed in GSE39582 data, which includes 566 cases with R value of 0.7268 (Figure 3G). In our own cohort, the expression of PCDH7 is also remarkable positively correlated with LNAPPCC with R value of 0.7308 (Figure 3H).

LNAPPCC Activates *PCDH7* Expression via Relieving the Repressive Roles of EZH2 on *PCDH7*

PCDH7 was previously reported as a polycomb group target gene.[28] EZH2 is the catalytic subunit of the polycomb repressive complex 2 (PRC2), which catalyzes trimethylation of histone H3 lysine 27 (H3K27me3).[29,30] H3K27me3 is a repressive chromatin marker and represses target gene transcription.[31] Intriguingly, an interaction between LNAPPCC and EZH2 was predicted by the online RNA-protein interaction prediction (RPISeq)[32] (http://pridb.gdcb.iastate.edu/RPISeq/) with random forest classifier value of 0.7 and support vector machine classifier value of 0.98 (greater than 0.5 was considered positive). Therefore, we hypothesized that whether the interaction between LNAPPCC and EZH2 regulates the transcription of *PCDH7*. RNA pull-down assays using biotin-labeled LNAPPCC were undertaken in SW620 and HCT116 cells. As shown in Figures 4A and S3A, EZH2 was remarkably enriched in biotin-labeled LNAPPCC group. Furthermore, RNA immunoprecipitation (RIP) assays using EZH2-specific antibody revealed that LNAPPCC was specifically enriched in EZH2 antibody group (Figure 4B). HOTAIR and GAPDH mRNA was used as positive and negative controls, respectively, for EZH2 binding (Figures S3B and S3C). Because EZH2 was reported to bind G-rich motif,[33] we next scanned for G-rich motif in LNAPPCC and identified a G-rich motif in 685–715 nt of LNAPPCC (Figure 4C). RIP assays showed that the mutation of the G-rich motif abolished the enrichment of LNAPPCC by EZH2 (Figure 4D). These data showed that LNAPPCC interacts with EZH2. Next, we investigated whether the interaction between LNAPPCC and EZH2 modulates the binding of EZH2 to *PCDH7* promoter and the chromatin structure at *PCDH7* promoter. Chromatin immunoprecipitation (ChIP) assays showed that ectopic expression of LNAPPCC repressed the binding of EZH2 to *PCDH7* promoter and reduced H3K27me3

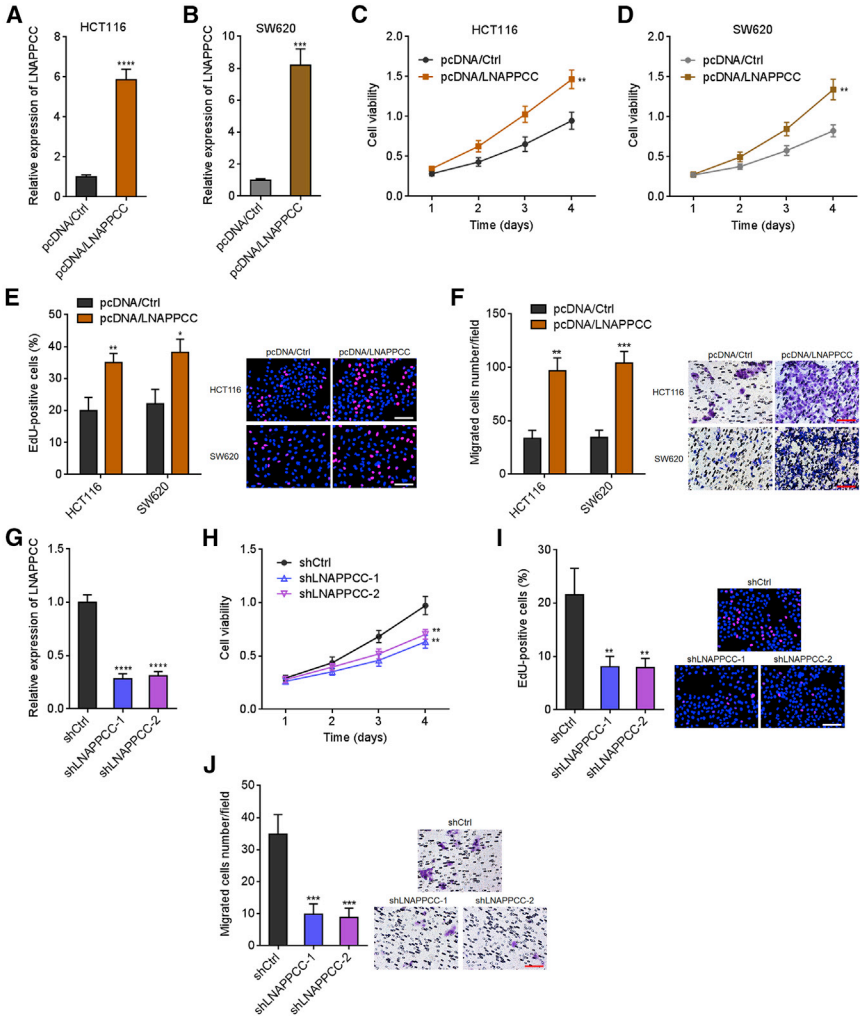

Figure 2. The Biological Roles of LNAPPCC in Colon Cancer Cell Proliferation and Migration

(A) LNAPPCC expression levels in LNAPPCC stably overexpressed and control HCT116 cells. (B) LNAPPCC expression levels in LNAPPCC stably overexpressed and control SW620 cells. (C) Cell proliferation of LNAPPCC stably overexpressed and control HCT116 cells was examined by CCK-8 assays. (D) Cell proliferation of LNAPPCC stably overexpressed and control SW620 cells was examined by CCK-8 assay. (E) Cell proliferation of LNAPPCC stably overexpressed and control HCT116 and SW620 cells was examined by EdU incorporation assay. Scale bars represent 100 μm. (F) Cell migration of LNAPPCC stably overexpressed and control HCT116 and SW620 cells was examined by Transwell migration assay. Scale bars represent 100 μm. (G) LNAPPCC expression levels in LNAPPCC stably silenced and control HCT116 cells. (H) Cell proliferation of LNAPPCC stably silenced and control HCT116 cells was examined by CCK-8 assay. (I) Cell proliferation of LNAPPCC stably silenced and control HCT116 cells was examined by EdU incorporation assay. Scale bars represent 100 μm. (J) Cell migration of LNAPPCC stably silenced and control HCT116 cells was examined by Transwell migration assay. Scale bars represent 100 μm. Data are presented as mean ± SD based on at least three independent biological repeats. *$p < 0.05$, **$p < 0.01$, ***$p < 0.001$, ****$p < 0.0001$, by Student's t test (A–F) or one-way ANOVA followed by Dunnett's multiple comparisons test (G–J).

level at *PCDH7* promoter (Figure 4E). Conversely, silencing of LNAPPCC increased the binding of EZH2 to *PCDH7* promoter and upregulated H3K27me3 level at *PCDH7* promoter (Figure 4F). *p16*, which was reported to be a target gene of EZH2, was used as control (Figures S3D and S3E). Then, the effects of LNAPPCC on *PCDH7* expression were detected. The mRNA and protein levels of PCDH7 were remarkably increased in LNAPPCC stably overexpressed HCT116 and SW620 cells (Figures 4G and 4H). Conversely, the mRNA and protein levels of PCDH7 were remarkably decreased in LNAPPCC stably silenced HCT116 cells (Figure 4I). Therefore, these findings suggested that LNAPPCC activates *PCDH7* expression via reducing the binding and repressive roles of EZH2 on PCDH7 *promoter*.

PCDH7 Promotes Colon Cancer Cell Proliferation and Migration

To investigate whether PCDH7 is a mediator of the oncogenic roles of LNAPPCC in colon cancer, we next examined the potential roles of PCDH7 in colon cancer. PCDH7 stably overexpressed HCT116 cells were constructed via stable transfection of PCDH7 mammalian expression plasmid pReceiver/PCDH7 (Figure 5A). CCK-8 and EdU incorporation assays both revealed that cell proliferation of HCT116 cells was remarkably increased by PCDH7 overexpression (Figures 5B and 5C). Transwell assays revealed that cell migration of HCT116 cells was also remarkably increased by PCDH7 overexpression (Figure 5D). PCDH7 stably silenced HCT116 cells were further constructed via stable transfection of two independent PCDH7-specific shRNAs (Figure 5E). Both CCK-8 and EdU incorporation assays revealed that cell proliferation was remarkably repressed by silencing of PCDH7 (Figures 5F and 5G). Transwell assays revealed that cell migration was also remarkably repressed by silencing of PCDH7 (Figure 5H). Therefore, these findings suggested that consistent with LNAPPCC, PCDH7 also plays oncogenic roles in colon cancer.

PCDH7 Increases *LNAPPCC* Expression via Activating ERK/c-FOS Signaling

Due to the significant positive correlation between the expression of PCDH7 and LNAPPCC in colon cancer tissues, we next investigated whether PCDH7 could modulate LNAPPCC expression inversely. The expression of LNAPPCC in PCDH7 stably overexpressed and silenced HCT116 cells was detected by quantitative real-time PCR. Intriguingly, LNAPPCC was remarkably increased in PCDH7 overexpressed cells and decreased in PCDH7 silenced cells (Figure 6A;

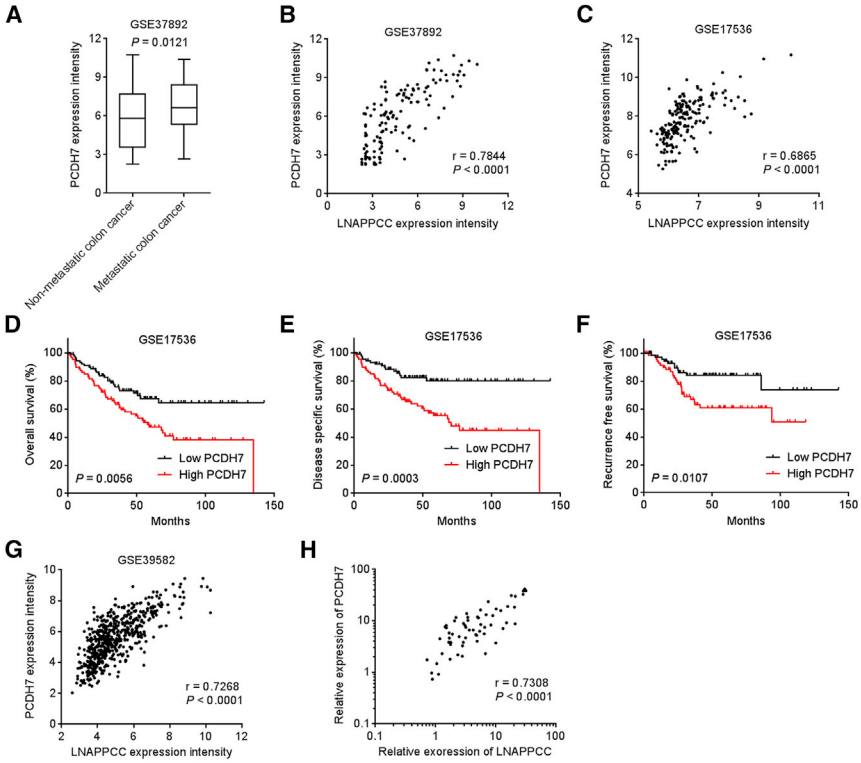

Figure 3. The Correlation between PCDH7 and LNAPPCC Expression in Colon Cancer Tissues

(A) PCDH7 expression intensities in 93 non-metastatic and 37 metastatic colon cancer tissues from GSE37892 data. p = 0.0121 by Mann-Whitney test. (B) The correlation between PCDH7 and LNAPPCC expression intensities from GSE37892 data. n = 130, r = 0.7844, p < 0.0001 by Spearman correlation analysis. (C) The correlation between PCDH7 and LNAPPCC expression intensities from GSE17536 data. n = 177, r = 0.6865, p < 0.0001 by Spearman correlation analysis. (D) Kaplan-Meier survival analysis of the correlation between PCDH7 expression intensities and overall survival from GSE17536 data. n = 177, p = 0.0056 by log-rank test. (E) Kaplan-Meier survival analysis of the correlation between PCDH7 expression intensities and disease specific survival from GSE17536 data. n = 177, p = 0.0003 by log-rank test. (F) Kaplan-Meier survival analysis of the correlation between LNAPPCC expression intensities and recurrence free survival from GSE17536 data. n = 145, p = 0.0107 by log-rank test. (G) The correlation between PCDH7 and LNAPPCC expression intensities from GSE39582 data. n = 566, r = 0.7268, p < 0.0001 by Spearman correlation analysis. (H) The correlation between PCDH7 and LNAPPCC expression levels in 62 colon cancer tissues. r = 0.7308, p < 0.0001 by Spearman correlation analysis.

Figure S4A). These data suggested that PCDH7 also upregulates LNAPPCC. Previous reports showed that PCDH7 activates mitogen-activated protein kinase (MAPK) signaling in lung cancer.[34,35] In this study, we further investigated whether PCDH7 also activates MAPK signaling in colon cancer. As shown in Figures 6B and S4B, ectopic expression of PCDH7 induced ERK and c-FOS activation, and conversely, silencing of PCDH7 repressed ERK and c-FOS activation in colon cancer cells. Searching *LNAPPCC* promoter, we identified a c-FOS binding site located at 460 bp upstream of LNAPPCC transcription initiation site (Figure 6C). Luciferase reporter assays showed that c-FOS increased LNAPPCC promoter activity (Figure 6D). ChIP assays showed that ectopic expression of PCDH7 increased the binding of c-FOS to *LNAPPCC* promoter, whereas silencing of PCDH7 decreased the binding of c-FOS to *LNAPPCC* promoter (Figure 6E; Figure S4C). To investigate whether the upregulation of LNAPPCC by PCDH7 is dependent on the activation of ERK/c-FOS signaling, we treated PCDH7 stably overexpressed HCT116 cells with ERK inhibitor GDC-0994. The results showed that inhibition of ERK activation abrogated the upregulation of LNAPPCC caused by PCDH7 overexpression (Figure 6F). Thus, these findings suggested that PCDH7 upregulates *LNAPPCC* expression via activating ERK/c-FOS signaling. Combined with the findings that LNAPPCC activates *PCDH7* expression, our data demonstrated that LNAPPCC/PCDH7/ERK/c-FOS form a positive feedback loop in colon cancer (Figure 6G). Via activating PCDH7/ERK/c-FOS axis, ectopic expression of LNAPPCC increased the binding of c-FOS to *LNAPPCC* promoter, whereas silencing of LNAPPCC decreased the binding of c-FOS to *LNAPPCC* promoter (Figure 6H; Figure S4D), which further support the LNAPPCC/PCDH7/ERK/c-FOS positive feedback loop. The correlations between LNAPPCC expression, PCDH7 expression, ERK activation, and c-FOS activation were further analyzed in colon cancer tissues. In our cohort containing 62 colon cancer cases, we found that the colon cancer tissues with strong phosphorylated ERK staining have higher expression of LNAPPCC and PCDH7 than the colon cancer tissues with weak phosphorylated ERK staining (Figures 6I and 6J). The colon cancer tissues with strong phosphorylated c-FOS staining also have higher expression of LNAPPCC and PCDH7 than the colon cancer tissues with weak phosphorylated c-FOS staining (Figures 6K and 6L).

ERK Inhibitor or Depletion of PCDH7 Abrogates the Roles of LNAPPCC in Promoting Colon Cancer Cell Proliferation and Migration

To examine whether LNAPPCC exerts oncogenic roles via the LNAPPCC/PCDH7/ERK/c-FOS feedback loop in colon cancer, we treated LNAPPCC stably overexpressed HCT116 cells with ERK inhibitor GDC-0994. CCK-8 and EdU incorporation assays revealed that the pro-proliferative roles of LNAPPCC were abolished by ERK inhibitor (Figures 7A and 7B). Transwell assays revealed that the pro-migratory roles of LNAPPCC were also abolished by ERK inhibitor (Figure 7C). In addition, PCDH7 was stably silenced in LNAPPCC stably overexpressed HCT116 cells via stable transfection of PCDH7-specific shRNA into LNAPPCC overexpressed HCT116 cells (Figure 7D). CCK-8 and EdU incorporation assays revealed

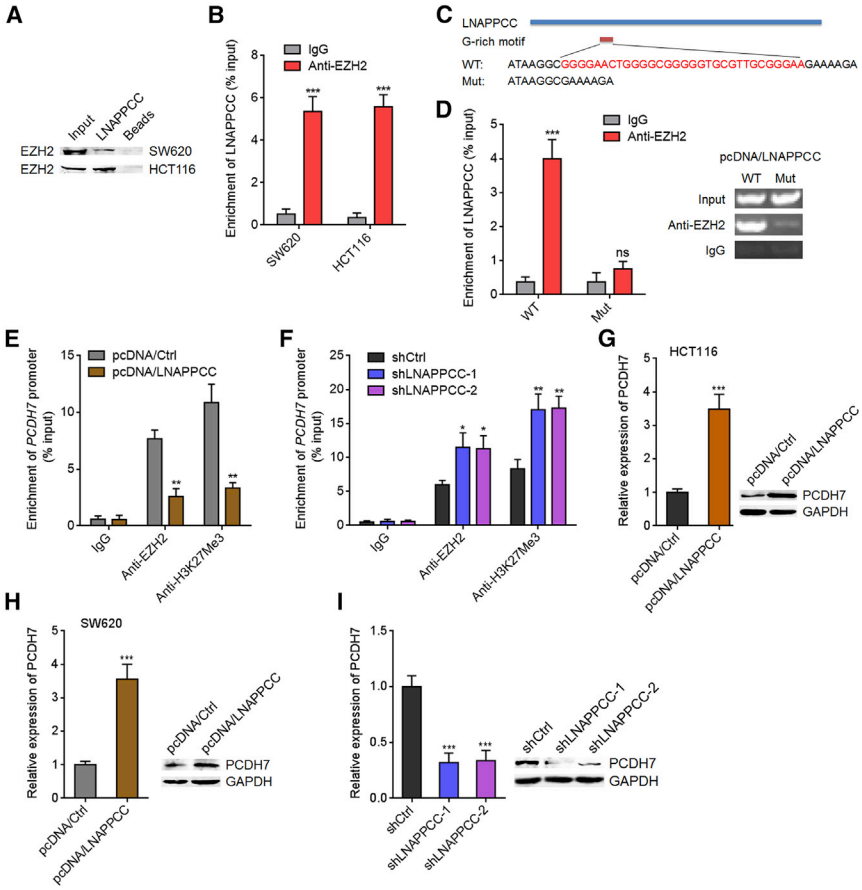

Figure 4. LNAPPCC Activates PCDH7 Expression via Binding EZH2

(A) RNA pull-down assay using biotin-labeled LNAPPCC was undertaken to detect the interaction between LNAPPCC and EZH2. (B) RIP assay using EZH2 specific antibody was undertaken to detect the binding between EZH2 and LNAPPCC. (C) Schematic outlining the predicted G-rich motif in LNAPPCC and the wild-type (WT) and mutated LNAPPCC sequences used for RIP with anti-EZH2. LNAPPCC-Mut contains a deletion of the G-rich motif. (D) After transient transfection of LNAPPCC-WT or LNAPPCC-Mut overexpression plasmids into HCT116 cells, RIP assay was undertaken using EZH2 specific antibody. (E) ChIP assay using EZH2 and H3K27me3 specific antibodies was undertaken in LNAPPCC stably overexpressed and control SW620 cells to detect the effects of LNAPPCC overexpression on the binding of EZH2 to *PCDH7* promoter and H3K27me3 level at *PCDH7* promoter. (F) ChIP assay using EZH2 and H3K27me3 specific antibodies was undertaken in LNAPPCC stably silenced and control HCT116 cells to detect the effects of LNAPPCC silencing on the binding of EZH2 to *PCDH7* promoter and H3K27me3 level at *PCDH7* promoter. (G) PCDH7 mRNA and protein levels in LNAPPCC stably overexpressed and control HCT116 cells were detected by quantitative real-time PCR and western blot. (H) PCDH7 mRNA and protein levels in LNAPPCC stably overexpressed and control SW620 cells were detected by quantitative real-time PCR and western blot. (I) PCDH7 mRNA and protein levels in LNAPPCC stably silenced and control HCT116 cells were detected by quantitative real-time PCR and western blot. Data are presented as mean ± SD based on at least three independent biological repeats. $^{*}p < 0.05$, $^{**}p < 0.01$, $^{***}p < 0.001$, ns, not significant, by Student's t test (B, D, E, G, and H) or one-way ANOVA followed by Dunnett's multiple comparisons test (F and I).

that the pro-proliferative roles of LNAPPCC were abolished by the silencing of PCDH7 (Figures 7E and 7F). Transwell assays revealed that the pro-migratory roles of LNAPPCC were also abolished by the silencing of PCDH7 (Figure 7G). Therefore, these findings suggested that LNAPPCC promotes colon cancer cell proliferation and migration via the positive LNAPPCC/PCDH7/ERK/c-FOS feedback loop.

LNAPPCC Facilitates Colon Cancer Xenograft Growth and Liver Metastasis in a PCDH7-Dependent Manner

To investigate the *in vivo* roles of LNAPPCC in colon cancer growth and metastasis, we subcutaneously injected LNAPPCC stably overexpressed HCT116 cells with or without PCDH7 silencing into nude mice. As shown in Figures 8A–8C, overexpression of LNAPPCC remarkably promoted colon cancer xenograft growth, which was abrogated by the silencing of PCDH7. Overexpression of LNAPPCC and PCDH7 in subcutaneous xenografts derived from LNAPPCC overexpressed HCT116 cells were confirmed (Figure 8D). Furthermore, the downregulation of LNAPPCC and PCDH7 in subcutaneous xenografts derived from PCDH7-silenced HCT116 cells were also confirmed (Figure 8D). Ki67 staining of subcutaneous xenografts revealed that overexpression of LNAPPCC promoted colon cancer cell proliferation *in vivo*, which was abolished by the silencing of PCDH7 (Figure 8E). Phosphorylated ERK and c-FOS staining revealed that overexpression of LNAPPCC activated ERK and c-FOS *in vivo*, which was also abolished by the silencing of PCDH7 (Figures 8F and 8G; Figures S5A and S5B). In addition, LNAPPCC stably overexpressed HCT116 cells with or without PCDH7 silencing were intrasplenically injected into nude mice to construct liver metastasis model. As shown in Figures 8H–8J, overexpression of LNAPPCC remarkably promoted colon cancer liver metastasis, which was abrogated by the silencing of PCDH7. To confirm the roles of LNAPPCC in colon cancer xenograft growth and liver metastasis, we subcutaneously injected LNAPPCC stably silenced HCT116 cells into nude mice. LNAPPCC knockdown remarkably repressed colon cancer xenograft growth (Figures S5C–S5E). Downregulation of LNAPPCC and PCDH7 in subcutaneous xenografts derived from LNAPPCC-silenced HCT116 cells were confirmed (Figure S5F). Ki67 staining of subcutaneous xenografts revealed that LNAPPCC knockdown repressed colon cancer cell proliferation *in vivo* (Figure S5G). Phosphorylated ERK and c-FOS staining revealed that LNAPPCC knockdown inactivated ERK and c-FOS *in vivo* (Figures S5H–S5K). In addition, LNAPPCC stably silenced HCT116 cells were intrasplenically injected into nude mice to construct liver metastasis model. As shown

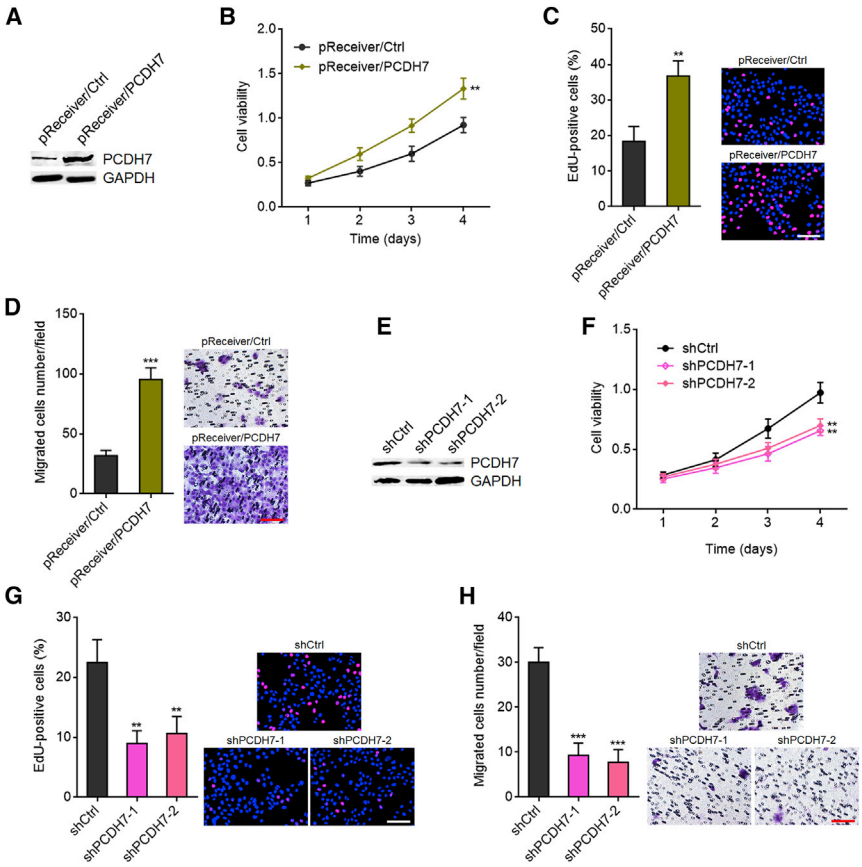

Figure 5. The Roles of PCDH7 in Colon Cancer Cell Proliferation and Migration

(A) PCDH7 expression levels in PCDH7 stably overexpressed and control HCT116 cells. (B) Cell proliferation of PCDH7 stably overexpressed and control HCT116 cells was examined by CCK-8 assays. (C) Cell proliferation of PCDH7 stably overexpressed and control HCT116 cells was examined by EdU incorporation assay. Scale bars represent 100 μm. (D) Cell migration of PCDH7 stably overexpressed and control HCT116 cells was examined by Transwell migration assay. Scale bars represent 100 μm. (E) PCDH7 expression levels in PCDH7 stably silenced and control HCT116 cells. (F) Cell proliferation of PCDH7 stably silenced and control HCT116 cells was examined by CCK-8 assay. (G) Cell proliferation of PCDH7 stably silenced and control HCT116 cells was examined by EdU incorporation assay. Scale bars represent 100 μm. (H) Cell migration of PCDH7 stably silenced and control HCT116 cells was examined by Transwell migration assay. Scale bars represent 100 μm. Data are presented as mean ± SD based on at least three independent biological repeats. $^{**}p < 0.01$, $^{***}p < 0.001$ by Student's t test (B–D) or one-way ANOVA followed by Dunnett's multiple comparisons test (F and H).

in Figure S5L–S5N, LNAPPCC knockdown remarkably inhibited colon cancer liver metastasis.

DISCUSSION

Until now, surgical resection is still the most efficient therapeutic strategy for most colon cancer. However, approximately 30% of colon cancer patients may suffer postoperative recurrence or metastasis.[5] Therefore, identifying predictive biomarkers for colon cancer recurrence and/or metastasis may be beneficial to the early intervention.[36] In this study, we first identified that lncRNA LNAPPCC is remarkably associated with colon cancer recurrence and metastasis using multiple cohorts. Our findings demonstrated that LNAPPCC is highly expressed in colon cancer tissues and cell lines. Increased expression of LNAPPCC is remarkably positively associated with metastasis, recurrence, and poor survival of colon cancer patients.

The gene encoding LNAPPCC is located at chromosome 11q24.1. LNAPPCC has one exon and 2,445 nucleotides in length. Except for the aberrant expression of LNAPPCC in colon cancer, LNAPPCC was also found to play critical roles in colon cancer. Gain-of-function experiments demonstrated that LNAPPCC promotes colon cancer cell proliferation and migration *in vitro* and colon cancer xenograft growth and liver metastasis *in vivo*. Loss-of-function experiments showed that silencing of LNAPPCC inhibits colon cancer cell proliferation and migration *in vitro* and colon cancer xenograft growth and liver metastasis *in vivo*. Thus, our data suggested that LNAPPCC has oncogenic roles in colon cancer and represents a potential therapeutic target for colon cancer.

Molecular mechanisms underlying the roles of lncRNAs are complex and various.[37–39] Different subcellular locations of lncRNAs implies different molecular mechanisms. For cytoplasmic lncRNAs, they could directly bind proteins, microRNAs (miRs), and/or mRNAs and change the modification, stability, location, and roles of the interacted partners.[40–42] For nuclear lncRNAs, one of the main mechanisms is to bind epigenetic modification machineries, modulate epigenetic modification and chromatin structure of target genes, and therefore modulate the expression of target genes.[43–45] Among the epigenetic modification machineries, PRC2, which catalyzes H3K27me3 and represses target genes expression, is frequently involved in the roles of lncRNAs.[46] Several lncRNAs, such as HOTAIR, ANCR, H19, SYISL, AFAP1-AS1 have been reported to bind EZH2, the catalytic subunit PRC2, change genomic location of EZH2, and therefore regulate the expression of target genes.[47–51] In this study, using bioinformatic analysis and experimental verification, we also found that LNAPPCC binds to EZH2. Although we identified the interaction between LNAPPCC and EZH2, whether the interaction is direct or indirect needs further investigation. In multiple cohorts, we found a remarkably positive correlation between the expression of LNAPPCC and PCDH7. PCDH7 has

been reported to be a PRC2 target. In this study, we further found that via interacting with EZH2, LNAPPCC suppresses the binding of EZH2 to *PCDH7* promoter, reduces H3K27me3 level at *PCDH7* promoter, and thus upregulates *PCDH7* expression. PCDH7, also known as protocadherin 7, belongs to the cadherin superfamily. PCDH7 has been reported to have oncogenic roles in lung cancer and breast cancer via activating MAPK or PLCβ-Ca^{2+}/CaMKII/S100A4 signaling.[26,34] In this study, we found that PCDH7 also plays oncogenic roles in colon cancer via activating MAPK-c-FOS signaling. Except PCDH7, whether LNAPPCC regulate the expression of other genes via interacting with EZH2 needs further investigation.

Except for the positive regulation of PCDH7 by LNAPPCC, we further found that PCDH7 could positively regulate LNAPPCC via activated ERK and c-FOS signaling. LNAPPCC was identified as a transcription target of c-FOS. Therefore, LNAPPCC, PCDH7, ERK, and c-FOS form a positive feedback loop. In clinical colon cancer tissues, we also found significant positive correlation between LNAPPPCC expression, PCDH7 expression, ERK phosphorylation level, and c-FOS phosphorylation level. The positive feedback loop could amplify the effects of participants. Several feedback loops have been reported to be employed by cancer cells to exert their malignant behaviors, such as ERIC/E2F, miR-200a/HDAC4, SNHG14/miR-5590-3p/ZEB1, NF90/lncRNA-LET/miR-548k, and so on.[52–55] Functional rescue experiments showed that inhibition of ERK activation or silencing of PCDH7 abrogated the oncogenic roles of LNAPPCC in colon cancer, which suggested that the LNAPPCC/PCDH7/ERK/c-FOS feedback loop at least partially mediates the oncogenic roles of LNAPPCC in colon cancer.

In summary, this study identified a novel oncogenic lncRNA LNAPPCC, which is upregulated in colon cancer and correlated with metastasis, recurrence, and poor prognosis of colon cancer patients. LNAPPCC facilitates colon cancer cell proliferation and migration *in vitro* and colon cancer growth and liver metastasis *in vivo* via activating the LNAPPCC/PCDH7/ERK/c-FOS positive feedback loop. Our findings suggested LNAPPCC as a potential predictive biomarker for colon cancer metastasis and recurrence. Our results also suggested that targeting LNAPPCC/EZH2/PCDH7/ERK/c-FOS feedback loop represents a potential therapeutic strategy for colon cancer.

MATERIALS AND METHODS

Clinical Samples

A total of 62 pairs of colon cancer tissues and matched adjacent normal tissues were collected from colon cancer patients who received surgery at Hainan General Hospital. Postoperatively, the clinical samples were histopathologically staged following the TNM system. The clinicopathological characteristics of these 62 colon cancer patients are shown in Table 1. Written informed consent was obtained from each patient. This study was carried out in accordance with the Declaration of Helsinki and approved by the Ethics Committee of Hainan General Hospital.

Cell Culture and Treatment

Normal human colon mucosal epithelial cell line NCM460 and colon cancer cell lines HT-29, SW620, HCT-15, and HCT116 were purchased from Cell Bank of Chinese Academy of Sciences (Shanghai, China). NCM460 cells were grown in Dulbecco's modified Eagle's medium (DMEM) (GIBCO). HT-29 and HCT116 cells were grown in McCoy's 5a medium (Sigma). SW620 cells were grown in L-15 medium (GIBCO). HCT-15 cells were grown in RPMI-1640 medium (GIBCO). All cells were cultured in the above described medium complemented with 10% fetal bovine serum (GIBCO) in a moist air with 5% CO_2 at 37°C. Where indicated, cells were treated with 1 μM GDC-0994 (Selleck) for the indicated time.

Quantitative Real-Time PCR

Total RNA was extracted from tissues and cells using RNAiso Plus (Takara) following the provided protocol. Subsequently, the RNA was reverse-transcribed into first strand complementary DNA (cDNA) with PrimeScript 1st strand cDNA Synthesis Kit (Takara). The cDNA was then used to undertake quantitative real-time PCR with TB Green Premix Ex Taq II (Takara) on StepOne Plus System (Applied Biosystems, Foster City, CA, USA). GAPDH was used as endogenous control. The primer sequences used for quantitative real-time PCR were as follows: for LNAPPCC: 5′-TTCGGACACAGAAGGACA-3′ (sense) and 5′-GGAAACAGAGGCAAAAAAG-3′ (antisense); for PCDH7: 5′-ATCTACCACCAGCCAACA-3′ (sense) and 5′-ACTCACAACAGAAAACGTCA-3′ (antisense); for HOTAIR: 5′-TTCCACAGACCAACACCC-3′ (sense) and 5′-CTAAATCCGTTCCATTCCA-3′ (antisense); for GAPDH: 5′-GGTCTCCTCTGACTTCAACA-3′ (sense) and 5′-GTGAGGGTCTCTCTCTTCCT-3′ (antisense); for β-actin: 5′-GGGAAATCGTGCGTGACATTAAG-3′ (sense) and 5′-TGTGTTGGCGTACAGGTCTTTG-3′ (antisense); and for U6: 5′-GCTTCGGCAGCACATATACTAAAAT-3′ (sense) and 5′-CGCTTCACGAATTTGCGTGTCAT-3′ (antisense). The relative expressions levels of RNAs were calculated by the $2^{-\Delta\Delta Ct}$ method.

Isolation of Cytoplasmic, Nuclear, and Poly(A)-Positive RNA

Cytoplasmic and nuclear fractions were isolated and harvested by the cytoplasmic and nuclear RNA purification kit (Norgen). The RNA present in the subcellular fractions was detected by quantitative real-time PCR. Poly(A)-positive RNA was enriched by the GenElute mRNA Miniprep Kit (Sigma) and then detected by quantitative real-time PCR.

5′ and 3′ Rapid Amplification of cDNA Ends (RACE)

The transcriptional initiation and termination sites of LNAPPCC were determined by 5′ and 3′ RACE analyses with SMARTer RACE cDNA Amplification Kit (Clontech) according to the manufacturer's manual. The primer sequences used for quantitative real-time PCR were as follows: for 5′ RACE, 5′-CCTGTTATCACTGAAAATCACGGAAGA-3′ and for 3′ RACE, 5′-CTGACTACACTACCGATGATGCTGGC-3′.

Plasmids Construction and Transfection

Full-length LNAPPCC was PCR-amplified from cDNA with the primers 5′-GGGGTACCTTTGATTGTCGAGTCATCGT-3′ (sense)

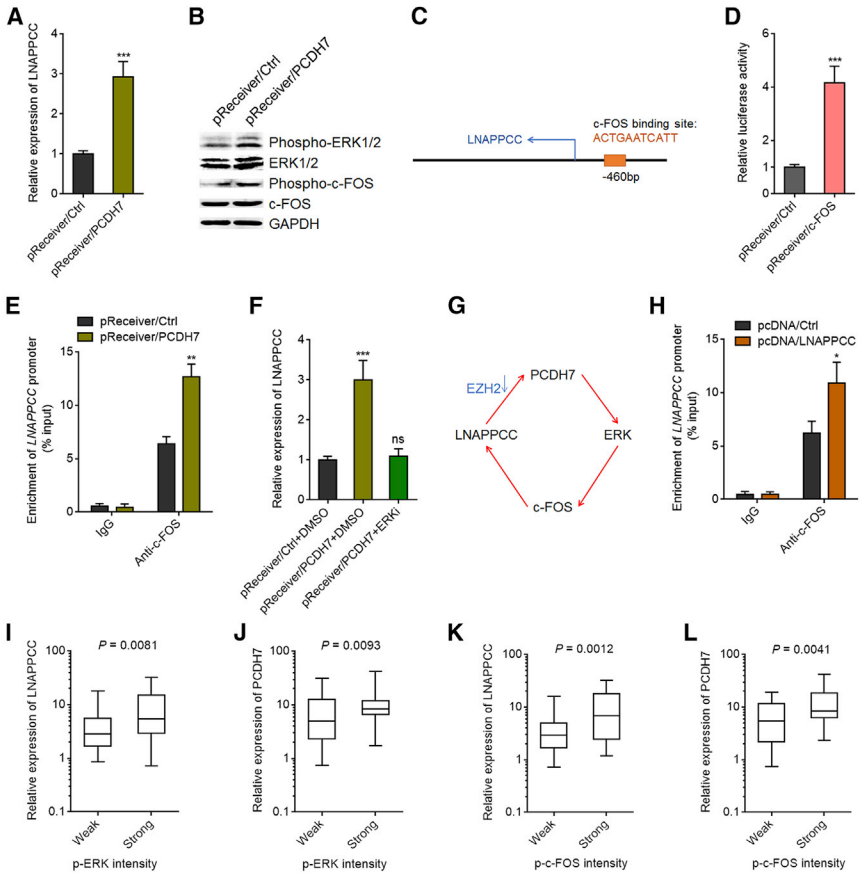

Figure 6. PCDH7 Upregulates LNAPPCC Expression via Activating ERK/c-FOS Signaling

(A) LNAPPCC expression levels in PCDH7 stably overexpressed and control HCT116 cells. (B) ERK and c-FOS phosphorylation levels in PCDH7 stably overexpressed and control HCT116 cells. (C) Schematic outlining the predicted binding site of c-FOS on *LNAPPCC* promoter. (D) After transient co-transfection of firefly luciferase reporter containing *LNAPPCC* promoter, pRL-TK (encoding renilla luciferase), and c-FOS overexpression plasmid into HCT116 cells, dual luciferase reporter assays were performed. Results were shown as relative ratio of firefly luciferase activity to renilla luciferase activity. (E) ChIP assay using c-FOS specific antibodies was undertaken in PCDH7 stably overexpressed and control HCT116 cells to detect the effects of PCDH7 overexpression on the binding of c-FOS to *LNAPPCC* promoter. (F) LNAPPCC expression levels in PCDH7 stably overexpressed HCT116 cells treated with 1 μM GDC-0994 for 48 h. (G) A schematic model of the LNAPPCC/PCDH7/ERK/c-FOS positive feedback loop. (H) ChIP assay using c-FOS specific antibodies was undertaken in LNAPPCC stably overexpressed and control HCT116 cells to detect the effects of LNAPPCC overexpression on the binding of c-FOS to *LNAPPCC* promoter. (I and J) LNAPPCC (I) and PCDH7 (J) expression levels in 62 colon cancer tissues with strong or weak p-ERK staining intensity. The median p-ERK staining intensity was used as the cutoff. p = 0.0081 (I) and p = 0.0093 (J) by Mann-Whitney test. (K and L) LNAPPCC (K) and PCDH7 (L) expression levels in 62 colon cancer tissues with strong or weak p-c-FOS staining intensity. The median p-c-FOS staining intensity was used as the cutoff. p = 0.0012 (K) and p = 0.0041 (L) by Mann-Whitney test. For (A), (D), (E), (F), and (H), data are presented as mean ± SD based on at least three independent biological repeats. *p < 0.05, **p < 0.01, ***p < 0.001, ns, not significant, by Student's t test (A, D, E, and H) or one-way ANOVA followed by Dunnett's multiple comparisons test (F).

and 5′-GGAATTCTCAGCAAGGAATGTCTTTAACAAG-3′ (antisense). Subsequently, the PCR products were subcloned into the KpnI and EcoR I sites of pCDNA3.1(+) backbone to construct LNAPPCC mammalian expression plasmid pcDNA/LNAPPCC. G-rich motif mutated LNAPPCC expression plasmid pcDNA/LNAPPCC-Mut (mutant) was synthesized by GenScript. Furthermore, the PCR products were also subcloned into the KpnI and EcoR I sites of pSPT19 backbone to construct LNAPPCC *in vitro* transcription plasmid pSPT19/LNAPPCC. Two independent cDNA oligonucleotides suppressing LNAPPCC expression (shLNAPPCC-1 and shLNAPPCC-2) were synthesized and inserted into the supersilencing shRNA expression vector pGPU6/Neo (GenePharma, Shanghai, China). A scrambled shRNA (shCtrl) was used as negative control. The shRNA sequences were as follows: for shLNAPPCC-1: 5′-CACCGCTGCCAAATTATACGAATGCTTCAAGAGAGCATTCGTATAATTTGGCAGCTTTTTTG-3′ (sense) and 5′-GATCCAAAAAAGCTGCCAAATTATACGAATGCTCTCTTGAAGCATTCGTATAATTTGGCAGC-3′ (antisense); for shLNAPPCC-2: 5′-CACCGGGCATTATTGATACTGATCTTTCAAGAGAAGATCAGTATCAATAATGCCCTTTTTTG-3′ (sense) and 5′-GATCCAAAAAAGGGCATTATTGATACTGATCTTCTCTTGAAAGATCAGTATCAATAATGCCC-3′ (antisense); for shCtrl: 5′-CACCGTTCTCCGAACGTGTCACGTCAAGAGATTACGTGACACGTTCGGAGAATTTTTTG-3′ (sense) and 5′-GATCCAAAAAATTCTCCGAACGTGTCACGTAATCTCTTGACGTGACACGTTCGGAGAAC-3′ (antisense). *LNAPPCC* promoter was PCR-amplified from DNA with the primers 5′-GGGGTACCATTGTTAGATGGGATCAGG-3′ (sense) and 5′-CCGCTCGAGGGACTATCAAAGACTGGA-3′ (antisense). Subsequently, the PCR products were subcloned into the KpnI and Xho I sites of pGL3-Basic vector (Promega) to construct firefly luciferase reporter containing *LNAPPCC* promoter. PCDH7 mammalian expression plasmid pReceiver/PCDH7 was purchased from GeneCopoeia (EX-Y4988-M02). c-FOS mammalian expression plasmid pReceiver/c-FOS was purchased from GeneCopoeia (EX-B0247-M02). The corresponding empty plasmid pReceiver-M02 was used as negative control. The shRNA suppressing PCDH7 expression (shPCDH7) was purchased from GeneCopoeia (HSH062195-mH1). The corresponding shRNA scrambled control was purchased from GeneCopoeia (CSHCTR001-mH1). Another shRNA targeting PCDH7 (shPCDH7-2) was purchased from GenePharma. Plasmids transfection was undertaken using Lipofectamine 3000 (Invitrogen) according to the manufacturer's manual.

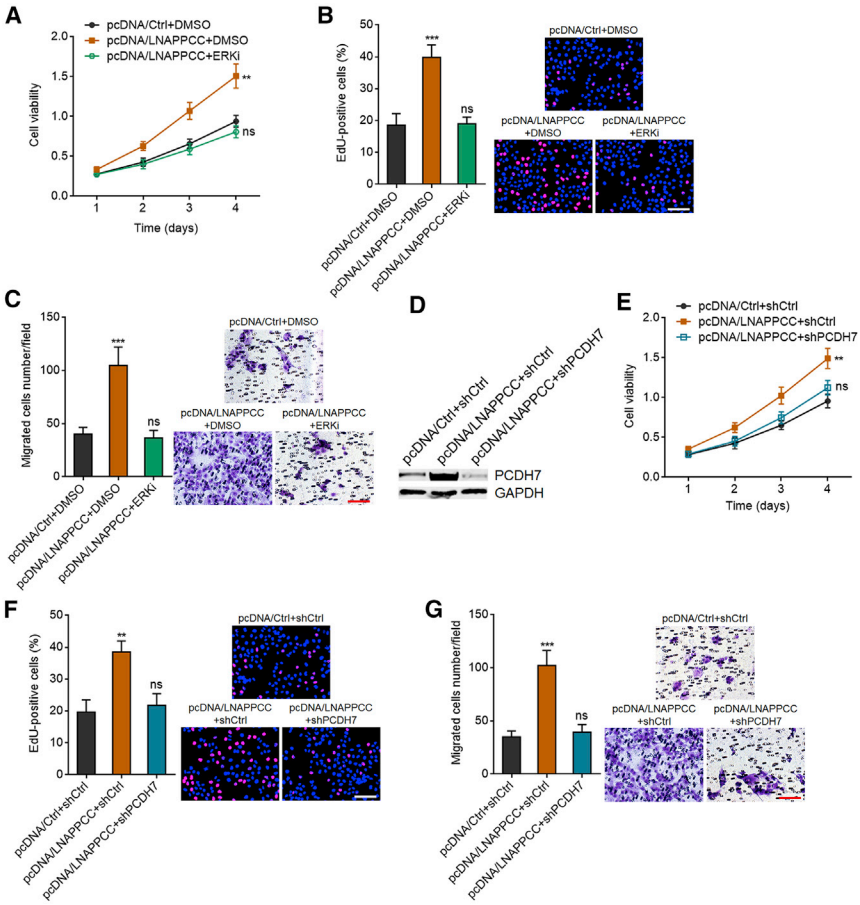

Figure 7. The Roles of LNAPPCC in Promoting Colon Cancer Cell Proliferation and Migration Are Dependent on the LNAPPCC/PCDH7/ERK/c-FOS Feedback Loop

(A) Cell proliferation of LNAPPCC stably overexpressed HCT116 cells treated with 1 μM GDC-0994 was examined by CCK-8 assays. (B) Cell proliferation of LNAPPCC stably overexpressed HCT116 cells treated with 1 μM GDC-0994 was examined by EdU incorporation assay. Scale bars represent 100 μm. (C) Cell migration of LNAPPCC stably overexpressed HCT116 cells treated with 1 μM GDC-0994 was examined by Transwell migration assay. Scale bars represent 100 μm. (D) PCDH7 expression levels in LNAPPCC stably overexpressed and concurrently PCDH7 stably silenced HCT116 cells. (E) Cell proliferation of LNAPPCC stably overexpressed and concurrently PCDH7 stably silenced HCT116 cells was examined by CCK-8 assays. (F) Cell proliferation of LNAPPCC stably overexpressed and concurrently PCDH7 stably silenced HCT116 cells was examined by EdU incorporation assay. Scale bars represent 100 μm. (G) Cell migration of LNAPPCC stably overexpressed and concurrently PCDH7 stably silenced HCT116 cells was examined by Transwell migration assay. Scale bars represent 100 μm. Data are presented as mean ± SD based on at least three independent biological repeats. $^{**}p < 0.01$, $^{***}p < 0.001$, ns, not significant, by one-way ANOVA followed by Dunnett's multiple comparisons test.

Cell Proliferation Assays

Cell proliferation was evaluated by CCK-8 and EdU incorporation assays. For CCK-8 assay, 2,000 indicated colon cancer cells/well were seeded into 96-well plates and cultured for 1, 2, 3, or 4 days. At indicated time, each well was added with 10 μL of CCK-8 reagent (Dojindo Laboratories) and incubated for another 2 h. Subsequently, the absorbance values at 450 nm were collected using a standard microplate reader. EdU incorporation assay was undertaken using the Cell-Light EdU *In Vitro* Kit (RiboBio) following the manufacturer's manual. The images of EdU-positive cells were collected using a fluorescence microscope (Carl Zeiss).

Cell Migration Assay

Cell migration was evaluated by Transwell migration assay. 50,000 indicated colon cancer cells were plated in the upper chamber of 24-well Transwell inserts (BD Biosciences) supplemented with serum-free medium. Lower chambers were added with medium supplemented with 10% fetal bovine serum (GIBCO). The inserts were further incubated in 5% CO_2 at 37°C for another 48 h. Then, the cells remaining on the upper chambers were removed, and the migratory cells were fixed and stained by crystal violet. The number of migratory cells was counted using a fluorescence microscope (Carl Zeiss).

RNA Pull-Down Assay

LNAPPCC was *in vitro* transcribed and biotinylated from pSPT19/LNAPPCC using Biotin RNA Labeling Mix (Roche) and T7 RNA polymerase (Roche) according to the manufacturer's manual. 3 μg of biotinylated and refolded LNAPPCC was incubated with 1 mg protein extracts from indicated colon cancer cells and Dynabeads Myone Streptavidin T1 beads (Invitrogen) overnight. Subsequently, the beads were washed three times. After streptavidin bead pull-down, the enriched proteins were detected by western blot.

Western Blot

Cells were lysed in radioimmunoprecipitation assay (RIPA) lysis buffer (Beyotime) added with protease inhibitor (Selleck) and phosphatase inhibitor (Selleck). The extracted or enriched proteins were separated by 12% SDS-PAGE. After being transferred into polyvinylidene fluoride (PVDF) membrane (Millipore), the blots were incubated with primary antibodies against EZH2 (1:500; 07-689; Millipore), PCDH7 (1:200; ab139274; Abcam), phospho-ERK1/2 (1:1,000; #4370; Cell Signaling Technology), ERK1/2 (1:1,000; #4695; Cell Signaling Technology), phospho-c-FOS (1:1,000; #5348; Cell Signaling Technology), c-FOS (1:1,000; #2250; Cell Signaling Technology), or GAPDH (1:10,000; T0004; Affinity). After three washes, the blots were further incubated with goat anti-mouse immunoglobulin G (IgG) H&L (IRDye 680RD) preadsorbed secondary antibody (1:10,000; ab216776; Abcam) or goat anti-rabbit IgG H&L (IRDye 800CW) preadsorbed secondary antibody (1:10,000;

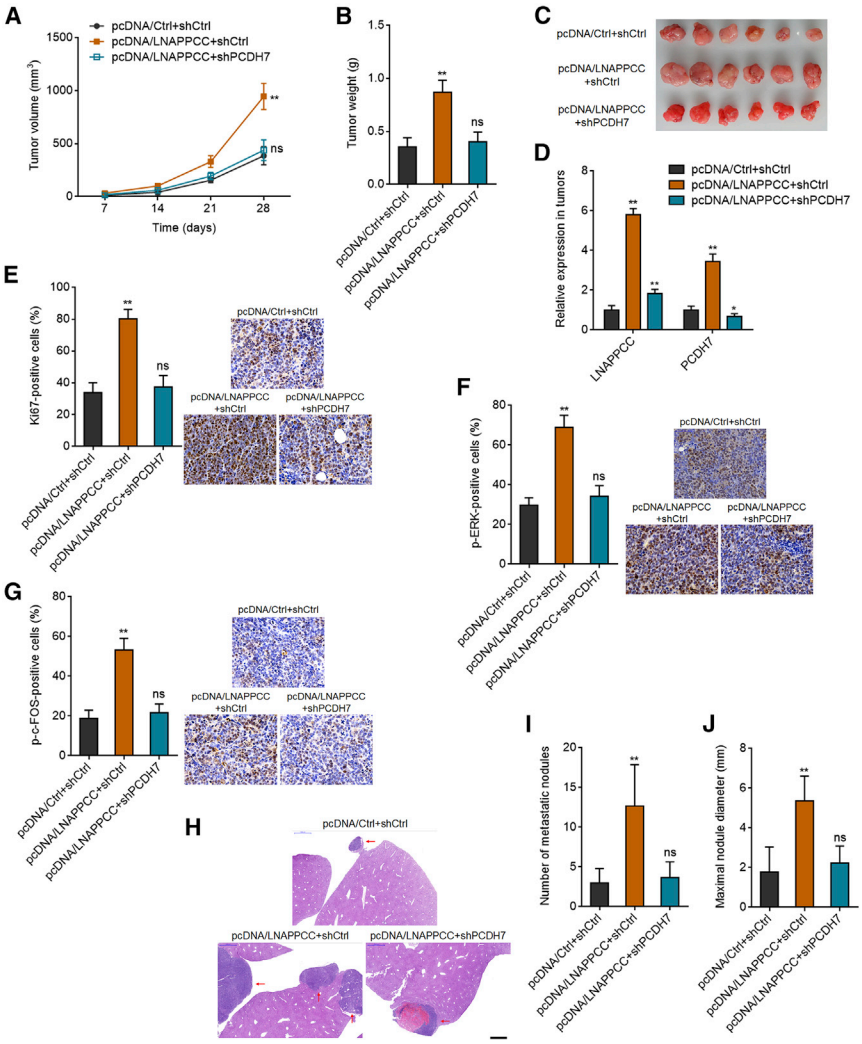

Figure 8. LNAPPCC Facilitates Colon Cancer Xenograft Growth and Liver Metastasis

(A) LNAPPCC stably overexpressed and concurrently PCDH7 stably silenced HCT116 cells were subcutaneously injected into nude mice. Subcutaneous tumor volumes were measured every 7 days. (B) Subcutaneous tumor weights were measured at the 28th day after injection. (C) Image of subcutaneous tumors excised at the 28th day after injection. (D) The expression of LNAPPCC and PCDH7 in subcutaneous tumors. (E) Ki67 IHC staining in subcutaneous tumors. (F) p-ERK IHC staining in subcutaneous tumors. (G) p-c-FOS IHC staining in subcutaneous tumors. (H–J) LNAPPCC stably overexpressed and concurrently PCDH7 stably silenced HCT116 cells were intrasplenically injected into nude mice. At the 35th day after injection, liver metastases of indicated colon cancer cells were detected by H&E staining. Scale bars represent 1,000 μm. Data are presented as mean ± SD based on n = 6 mice in each group. *$p < 0.05$, **$p < 0.01$, ns, not significant, by Kruskal-Wallis test followed by Dunn's multiple comparisons test.

ab216773; Abcam). The western blot images were obtained using Odyssey infrared scanner (Li-Cor).

RIP

RIP experiment was undertaken with the EZ-Magna RIP RNA-binding protein immunoprecipitation kit (Millipore) and EZH2 specific antibody (5 μg; 07-689; Millipore) following the manufacturer's manual. Enriched RNA was measured by quantitative real-time PCR.

ChIP

ChIP experiment was undertaken with the EZ-Magna ChIP A/G chromatin immunoprecipitation kit (Millipore) and specific antibodies against EZH2 (5 μg; 07-689; Millipore), H3K27me3 (5 μg; ab6002; Abcam), or Phospho-c-FOS (5 μg; #5348; Cell Signaling Technology) following the manufacturer's manual. Enriched DNA was measured by quantitative real-time PCR. The primer sequences were as follows: for *PCDH7* promoter: 5′-TTTGTTAATTGC CGTTGGGG-3′ (sense) and 5′-TCTTGCACGCTCTCTCTCC-3′ (antisense); for *LNAPPCC* promoter: 5′-ATAA CACCCAAACTGTAC-3′ (sense) and 5′-GGCC CAATAATACGAAAA-3′ (antisense); for *p16* promoter: 5′-GCCCAGTCCTCCTTCCTT-3′ (sense) and 5′-CCCTGTCCCTCAAATCCTC-3′ (antisense).

Luciferase Reporter Assay

c-FOS overexpression plasmid, firefly luciferase reporter containing *LNAPPCC* promoter, and pRL-TK plasmid that expressed renilla luciferase were co-transfected into HCT116 cells. 48 h after transfection, the luciferase activities were measured by Dual-Luciferase Reporter Assay System (Promega). The relative firefly luciferase activity was normalized to renilla luciferase activity.

Xenograft Experiment

Indicated colon cancer cells (5×10^6) were subcutaneously injected into 5- to 6-week-old athymic BALB/c nude mice. Subcutaneous xenograft growth was recorded every 7 days with a caliper, and tumor volume was calculated as $0.5 \times a \times b^2$ (a, longest diameter; b, shortest diameter). At the 28th day after injection, the mice were sacrificed and the subcutaneous tumors were resected, photographed, and weighed. For liver metastasis experiment, indicated colon cancer cells (2×10^6) were intrasplenically injected into 5- to 6-week-old athymic BALB/c nude mice. At the 35th day after injection, the mice were sacrificed and the livers were resected. The metastatic nodules were detected by hematoxylin and eosin (H&E) staining. Xenograft experiments were approved by the Ethics Committee of Hainan General Hospital.

Immunohistochemistry (IHC)

Subcutaneous xenograft and human colon cancer tissues were formalin-fixed and paraffin-embedded. Paraffin sections were used to perform Ki67, phospho-ERK1/2, ERK1/2, phospho-c-FOS, c-FOS IHC staining with primary antibodies against Ki67 (1:200; ab16667; Abcam), phospho-ERK1/2 (1:400; #4370; Cell Signaling Technology), ERK1/2 (1:250; #4695; Cell Signaling Technology), phospho-c-FOS (1:100; ab63444; Abcam), or c-FOS (1:1,000; ab208942; Abcam). After washes, the sections were further incubated with a horseradish peroxidase-conjugated anti-rabbit secondary antibody and visualized with 3,3-diaminobenzidine.

Statistical Analysis

Statistical analysis was undertaken using GraphPad Prism 6 software. Comparisons were calculated using Mann-Whitney test, Wilcoxon matched-pairs signed rank test, Pearson chi-square test, log-rank test, Student's t test, and one-way analysis of variance (ANOVA) followed by Dunnett's multiple comparisons test, Spearman correlation analysis, or Kruskal-Wallis test followed by Dunn's multiple comparisons test as indicated in the figure legends. p value < 0.05 was considered significant.

SUPPLEMENTAL INFORMATION

Supplemental Information can be found online at https://doi.org/10.1016/j.omtn.2020.03.017.

AUTHOR CONTRIBUTIONS

B.W., T.L., and Z.L. designed the study; T.L., Z.L., H.Wan, X.T., H. Wang, F.C., and M.Z. contributed to acquisition, analysis, and interpretation of the data; B.W. and T.L. drafted the manuscript; all authors gave final approval of the work.

CONFLICTS OF INTEREST

The authors declare no competing interests.

ACKNOWLEDGMENTS

This research was funded by Key Research Program of Hainan Province in Social Development (ZDYF2017090). The data that support the findings of this study are available on reasonable request from the corresponding author.

REFERENCES

1. Torre, L.A., Bray, F., Siegel, R.L., Ferlay, J., Lortet-Tieulent, J., and Jemal, A. (2015). Global cancer statistics, 2012. CA Cancer J. Clin. *65*, 87–108.
2. Bray, F., Ferlay, J., Soerjomataram, I., Siegel, R.L., Torre, L.A., and Jemal, A. (2018). Global cancer statistics 2018: GLOBOCAN estimates of incidence and mortality worldwide for 36 cancers in 185 countries. CA Cancer J. Clin. *68*, 394–424.
3. Siegel, R.L., Miller, K.D., and Jemal, A. (2019). Cancer statistics, 2019. CA Cancer J. Clin. *69*, 7–34.
4. Grothey, A., Sobrero, A.F., Shields, A.F., Yoshino, T., Paul, J., Taieb, J., Souglakos, J., Shi, Q., Kerr, R., Labianca, R., et al. (2018). Duration of Adjuvant Chemotherapy for Stage III Colon Cancer. N. Engl. J. Med. *378*, 1177–1188.
5. Böckelman, C., Engelmann, B.E., Kaprio, T., Hansen, T.F., and Glimelius, B. (2015). Risk of recurrence in patients with colon cancer stage II and III: a systematic review and meta-analysis of recent literature. Acta Oncol. *54*, 5–16.
6. Liu, Y., Sethi, N.S., Hinoue, T., Schneider, B.G., Cherniack, A.D., Sanchez-Vega, F., Seoane, J.A., Farshidfar, F., Bowlby, R., Islam, M., et al. (2018). Comparative Molecular Analysis of Gastrointestinal Adenocarcinomas. Cancer Cell *33*, 721–735.
7. Kong, X., Chen, J., Xie, W., Brown, S.M., Cai, Y., Wu, K., Fan, D., Nie, Y., Yegnasubramanian, S., Tiedemann, R.L., et al. (2019). Defining UHRF1 Domains that Support Maintenance of Human Colon Cancer DNA Methylation and Oncogenic Properties. Cancer Cell *35*, 633–648.
8. Iyer, M.K., Niknafs, Y.S., Malik, R., Singhal, U., Sahu, A., Hosono, Y., Barrette, T.R., Prensner, J.R., Evans, J.R., Zhao, S., et al. (2015). The landscape of long noncoding RNAs in the human transcriptome. Nat. Genet. *47*, 199–208.
9. Kim, E.S., Choi, J.Y., Hwang, S.J., and Bae, I.H. (2019). Hypermethylation of miR-205-5p by IR Governs Aggressiveness and Metastasis via Regulating Bcl-w and Src. Mol. Ther. Nucleic Acids *14*, 450–464.
10. Nuzzo, S., Catuogno, S., Capuozzo, M., Fiorelli, A., Swiderski, P., Boccella, S., de Nigris, F., and Esposito, C.L. (2019). Axl-Targeted Delivery of the Oncosuppressor miR-137 in Non-small-Cell Lung Cancer. Mol. Ther. Nucleic Acids *17*, 256–263.
11. Fatica, A., and Bozzoni, I. (2014). Long non-coding RNAs: new players in cell differentiation and development. Nat. Rev. Genet. *15*, 7–21.
12. Yuan, J.H., Yang, F., Wang, F., Ma, J.Z., Guo, Y.J., Tao, Q.F., Liu, F., Pan, W., Wang, T.T., Zhou, C.C., et al. (2014). A long noncoding RNA activated by TGF-β promotes the invasion-metastasis cascade in hepatocellular carcinoma. Cancer Cell *25*, 666–681.
13. Berger, A.C., Korkut, A., Kanchi, R.S., Hegde, A.M., Lenoir, W., Liu, W., Liu, Y., Fan, H., Shen, H., Ravikumar, V., et al. (2018). A Comprehensive Pan-Cancer Molecular Study of Gynecologic and Breast Cancers. Cancer Cell *33*, 690–705.
14. Arshi, A., Sharifi, F.S., Khorramian Ghahfarokhi, M., Faghih, Z., Doosti, A., Ostovari, S., Mahmoudi Maymand, E., and Ghahramani Seno, M.M. (2018). Expression Analysis of MALAT1, GAS5, SRA, and NEAT1 lncRNAs in Breast Cancer Tissues from Young Women and Women over 45 Years of Age. Mol. Ther. Nucleic Acids *12*, 751–757.
15. Barbagallo, C., Brex, D., Caponnetto, A., Cirnigliaro, M., Scalia, M., Magnano, A., Caltabiano, R., Barbagallo, D., Biondi, A., Cappellani, A., et al. (2018). LncRNA UCA1, Upregulated in CRC Biopsies and Downregulated in Serum Exosomes, Controls mRNA Expression by RNA-RNA Interactions. Mol. Ther. Nucleic Acids *12*, 229–241.
16. Hu, W.L., Jin, L., Xu, A., Wang, Y.F., Thorne, R.F., Zhang, X.D., and Wu, M. (2018). GUARDIN is a p53-responsive long non-coding RNA that is essential for genomic stability. Nat. Cell Biol. *20*, 492–502.
17. Chen, F., Chen, J., Yang, L., Liu, J., Zhang, X., Zhang, Y., Tu, Q., Yin, D., Lin, D., Wong, P.P., et al. (2019). Extracellular vesicle-packaged HIF-1α-stabilizing lncRNA from tumour-associated macrophages regulates aerobic glycolysis of breast cancer cells. Nat. Cell Biol. *21*, 498–510.
18. Esposito, R., Bosch, N., Lanzós, A., Polidori, T., Pulido-Quetglas, C., and Johnson, R. (2019). Hacking the Cancer Genome: Profiling Therapeutically Actionable Long Non-coding RNAs Using CRISPR-Cas9 Screening. Cancer Cell *35*, 545–557.
19. Wang, Z., Yang, B., Zhang, M., Guo, W., Wu, Z., Wang, Y., Jia, L., Li, S.; Cancer Genome Atlas Research Network, and Xie, W., et al. (2018). lncRNA Epigenetic Landscape Analysis Identifies EPIC1 as an Oncogenic lncRNA that Interacts with MYC and Promotes Cell-Cycle Progression in Cancer. Cancer Cell *33*, 706–720.
20. Mondal, T., Juvvuna, P.K., Kirkeby, A., Mitra, S., Kosalai, S.T., Traxler, L., Hertwig, F., Wernig-Zorc, S., Miranda, C., Deland, L., et al. (2018). Sense-Antisense lncRNA Pair Encoded by Locus 6p22.3 Determines Neuroblastoma Susceptibility via the USP36-CHD7-SOX9 Regulatory Axis. Cancer Cell *33*, 417–434.
21. Li, J.K., Chen, C., Liu, J.Y., Shi, J.Z., Liu, S.P., Liu, B., Wu, D.S., Fang, Z.Y., Bao, Y., Jiang, M.M., et al. (2017). Long noncoding RNA MRCCAT1 promotes metastasis of clear cell renal cell carcinoma via inhibiting NPR3 and activating p38-MAPK signaling. Mol. Cancer *16*, 111.
22. Liang, C., Zhao, T., Li, H., He, F., Zhao, X., Zhang, Y., Chu, X., Hua, C., Qu, Y., Duan, Y., et al. (2019). Long Non-coding RNA ITIH4-AS1 Accelerates the Proliferation and Metastasis of Colorectal Cancer by Activating JAK/STAT3 Signaling. Mol. Ther. Nucleic Acids *18*, 183–193.

23. Zhao, Y., Du, T., Du, L., Li, P., Li, J., Duan, W., Wang, Y., and Wang, C. (2019). Long noncoding RNA LINC02418 regulates MELK expression by acting as a ceRNA and may serve as a diagnostic marker for colorectal cancer. Cell Death Dis. *10*, 568.

24. Kawasaki, Y., Miyamoto, M., Oda, T., Matsumura, K., Negishi, L., Nakato, R., Suda, S., Yokota, N., Shirahige, K., and Akiyama, T. (2019). The novel lncRNA CALIC up-regulates AXL to promote colon cancer metastasis. EMBO Rep. *20*, e47052.

25. Li, A.M., Tian, A.X., Zhang, R.X., Ge, J., Sun, X., and Cao, X.C. (2013). Protocadherin-7 induces bone metastasis of breast cancer. Biochem. Biophys. Res. Commun. *436*, 486–490.

26. Ren, D., Zhu, X., Kong, R., Zhao, Z., Sheng, J., Wang, J., Xu, X., Liu, J., Cui, K., Zhang, X.H., et al. (2018). Targeting Brain-Adaptive Cancer Stem Cells Prohibits Brain Metastatic Colonization of Triple-Negative Breast Cancer. Cancer Res. *78*, 2052–2064.

27. Chen, Q., Boire, A., Jin, X., Valiente, M., Er, E.E., Lopez-Soto, A., Jacob, L., Patwa, R., Shah, H., Xu, K., et al. (2016). Carcinoma-astrocyte gap junctions promote brain metastasis by cGAMP transfer. Nature *533*, 493–498.

28. Beukers, W., Hercegovac, A., Vermeij, M., Kandimalla, R., Blok, A.C., van der Aa, M.M., Zwarthoff, E.C., and Zuiverloon, T.C. (2013). Hypermethylation of the polycomb group target gene PCDH7 in bladder tumors from patients of all ages. J. Urol. *190*, 311–316.

29. Rondinelli, B., Gogola, E., Yücel, H., Duarte, A.A., van de Ven, M., van der Sluijs, R., Konstantinopoulos, P.A., Jonkers, J., Ceccaldi, R., Rottenberg, S., and D'Andrea, A.D. (2017). EZH2 promotes degradation of stalled replication forks by recruiting MUS81 through histone H3 trimethylation. Nat. Cell Biol. *19*, 1371–1378.

30. Booth, C.A.G., Barkas, N., Neo, W.H., Boukarabila, H., Soilleux, E.J., Giotopoulos, G., Giotopoulos, G., Farnoud, N., Giustacchini, A., Ashley, N., Carrelha, J., et al. (2018). Ezh2 and Runx1 Mutations Collaborate to Initiate Lympho-Myeloid Leukemia in Early Thymic Progenitors. Cancer Cell *33*, 274–291.

31. Burr, M.L., Sparbier, C.E., Chan, K.L., Chan, Y.C., Kersbergen, A., Lam, E.Y.N., Azidis-Yates, E., Vassiliadis, D., Bell, C.C., Gilan, O., et al. (2019). An Evolutionarily Conserved Function of Polycomb Silences the MHC Class I Antigen Presentation Pathway and Enables Immune Evasion in Cancer. Cancer Cell *36*, 385–401.

32. Muppirala, U.K., Honavar, V.G., and Dobbs, D. (2011). Predicting RNA-protein interactions using only sequence information. BMC Bioinformatics *12*, 489.

33. You, B.H., Yoon, J.H., Kang, H., Lee, E.K., Lee, S.K., and Nam, J.W. (2019). HERES, a lncRNA that regulates canonical and noncanonical Wnt signaling pathways via interaction with EZH2. Proc. Natl. Acad. Sci. USA *116*, 24620–24629.

34. Zhou, X., Updegraff, B.L., Guo, Y., Peyton, M., Girard, L., Larsen, J.E., Xie, X.J., Zhou, Y., Hwang, T.H., Xie, Y., et al. (2017). PROTOCADHERIN 7 Acts through SET and PP2A to Potentiate MAPK Signaling by EGFR and KRAS during Lung Tumorigenesis. Cancer Res. *77*, 187–197.

35. Zhou, X., Padanad, M.S., Evers, B.M., Smith, B., Novaresi, N., Suresh, S., Richardson, J.A., Stein, E., Zhu, J., Hammer, R.E., and O'Donnell, K.A. (2019). Modulation of Mutant $Kras^{G12D}$ -Driven Lung Tumorigenesis *In Vivo* by Gain or Loss of PCDH7 Function. Mol. Cancer Res. *17*, 594–603.

36. Schild, T., Low, V., Blenis, J., and Gomes, A.P. (2018). Unique Metabolic Adaptations Dictate Distal Organ-Specific Metastatic Colonization. Cancer Cell *33*, 347–354.

37. Zhang, C., Yuan, J., Hu, H., Chen, W., Liu, M., Zhang, J., Sun, S., and Guo, Z. (2017). Long non-coding RNA CHCHD4P4 promotes epithelial-mesenchymal transition and inhibits cell proliferation in calcium oxalate-induced kidney damage. Braz. J. Med. Biol. Res. *51*, e6536.

38. Xu, M., Xu, X., Pan, B., Chen, X., Lin, K., Zeng, K., Liu, X., Xu, T., Sun, L., Qin, J., et al. (2019). LncRNA SATB2-AS1 inhibits tumor metastasis and affects the tumor immune cell microenvironment in colorectal cancer by regulating SATB2. Mol. Cancer *18*, 135.

39. Keshavarz, M., and Asadi, M.H. (2019). Long non-coding RNA ES1 controls the proliferation of breast cancer cells by regulating the Oct4/Sox2/miR-302 axis. FEBS J. *286*, 2611–2623.

40. Yuan, J.H., Liu, X.N., Wang, T.T., Pan, W., Tao, Q.F., Zhou, W.P., Wang, F., and Sun, S.H. (2017). The MBNL3 splicing factor promotes hepatocellular carcinoma by increasing PXN expression through the alternative splicing of lncRNA-PXN-AS1. Nat. Cell Biol. *19*, 820–832.

41. Chen, J., Yu, Y., Li, H., Hu, Q., Chen, X., He, Y., Xue, C., Ren, F., Ren, Z., Li, J., et al. (2019). Long non-coding RNA PVT1 promotes tumor progression by regulating the miR-143/HK2 axis in gallbladder cancer. Mol. Cancer *18*, 33.

42. Shen, W., Huang, B., He, Y., Shi, L., and Yang, J. (2019). Long non-coding RNA RP11-820 promotes extracellular matrix production via regulating miR-3178/MYOD1 in human trabecular meshwork cells. FEBS J. *287*, 978–990.

43. Zhu, X.T., Yuan, J.H., Zhu, T.T., Li, Y.Y., and Cheng, X.Y. (2016). Long noncoding RNA glypican 3 (GPC3) antisense transcript 1 promotes hepatocellular carcinoma progression via epigenetically activating GPC3. FEBS J. *283*, 3739–3754.

44. Zhai, W., Zhu, R., Ma, J., Gong, D., Zhang, H., Zhang, J., Chen, Y., Huang, Y., Zheng, J., and Xue, W. (2019). A positive feed-forward loop between LncRNA-URRCC and EGFL7/P-AKT/FOXO3 signaling promotes proliferation and metastasis of clear cell renal cell carcinoma. Mol. Cancer *18*, 81.

45. Zhang, L., Yang, F., Yuan, J.H., Yuan, S.X., Zhou, W.P., Huo, X.S., Xu, D., Bi, H.S., Wang, F., and Sun, S.H. (2013). Epigenetic activation of the MiR-200 family contributes to H19-mediated metastasis suppression in hepatocellular carcinoma. Carcinogenesis *34*, 577–586.

46. Wu, L., Murat, P., Matak-Vinkovic, D., Murrell, A., and Balasubramanian, S. (2013). Binding interactions between long noncoding RNA HOTAIR and PRC2 proteins. Biochemistry *52*, 9519–9527.

47. Wu, Y., Zhang, L., Zhang, L., Wang, Y., Li, H., Ren, X., Wei, F., Yu, W., Liu, T., Wang, X., et al. (2015). Long non-coding RNA HOTAIR promotes tumor cell invasion and metastasis by recruiting EZH2 and repressing E-cadherin in oral squamous cell carcinoma. Int. J. Oncol. *46*, 2586–2594.

48. Zhu, L., and Xu, P.C. (2013). Downregulated LncRNA-ANCR promotes osteoblast differentiation by targeting EZH2 and regulating Runx2 expression. Biochem. Biophys. Res. Commun. *432*, 612–617.

49. Luo, M., Li, Z., Wang, W., Zeng, Y., Liu, Z., and Qiu, J. (2013). Long non-coding RNA H19 increases bladder cancer metastasis by associating with EZH2 and inhibiting E-cadherin expression. Cancer Lett. *333*, 213–221.

50. Jin, J.J., Lv, W., Xia, P., Xu, Z.Y., Zheng, A.D., Wang, X.J., Wang, S.S., Zeng, R., Luo, H.M., Li, G.L., and Zuo, B. (2018). Long noncoding RNA *SYISL* regulates myogenesis by interacting with polycomb repressive complex 2. Proc. Natl. Acad. Sci. USA *115*, E9802–E9811.

51. Yin, D., Lu, X., Su, J., He, X., De, W., Yang, J., Li, W., Han, L., and Zhang, E. (2018). Long noncoding RNA AFAP1-AS1 predicts a poor prognosis and regulates non-small cell lung cancer cell proliferation by epigenetically repressing p21 expression. Mol. Cancer *17*, 92.

52. Feldstein, O., Nizri, T., Doniger, T., Jacob, J., Rechavi, G., and Ginsberg, D. (2013). The long non-coding RNA ERIC is regulated by E2F and modulates the cellular response to DNA damage. Mol. Cancer *12*, 131.

53. Yuan, J.H., Yang, F., Chen, B.F., Lu, Z., Huo, X.S., Zhou, W.P., Wang, F., and Sun, S.H. (2011). The histone deacetylase 4/SP1/microrna-200a regulatory network contributes to aberrant histone acetylation in hepatocellular carcinoma. Hepatology *54*, 2025–2035.

54. Zhao, L., Liu, Y., Zhang, J., Liu, Y., and Qi, Q. (2019). LncRNA SNHG14/miR-5590-3p/ZEB1 positive feedback loop promoted diffuse large B cell lymphoma progression and immune evasion through regulating PD-1/PD-L1 checkpoint. Cell Death Dis. *10*, 731.

55. Lin, J., Chen, Z., Wu, S., Huang, W., Chen, F., and Huang, Z. (2019). An NF90/long noncoding RNA-LET/miR-548k feedback amplification loop controls esophageal squamous cell carcinoma progression. J. Cancer *10*, 5139–5152.